

Anti-Personnel Mine Detection by Neutron Backscattering Technique Using MCNP Simulation

A. M. Ali^{1,2}

¹*Reactor Physics Department, Nuclear Research Centre, Atomic Energy Authority, Cairo, Egypt*

²*Physics Department, Faculty of Science, Jazan University, Saudi Arabia*

Received: 2/6/2015

Accepted: 3/8/2015

ABSTRACT

The neutron backscattering technique NBS has been applied for landmine detection if the soil is sufficiently dry. The detection of anti-personnel (AP) landmine by neutron backscattering technique has been studied by using Monte Carlo N-Particle (MCNP4B) code. The effect of the burial depth and side position of anti-personnel landmine has been discussed. A two dimensional position sensitive detector is simulated by MCNP4B to obtain an image of the back scattered slow neutrons radiation. Results of simulation using mono-energetic point neutron source (2.45 MeV) are presented. The on-mine to no-mine signal ratio images are presented for different positions and depths.

Key words: Anti-Personnel Landmine, neutron backscattering, position sensitive detector

INTRODUCTION

One of the proposed methods to search for low-metallic buried landmines is the neutron backscattering (NBS) technique ⁽¹⁾. In this technique the soil volume under investigation is irradiated with fast neutrons emitted from one of the isotopic neutron source or sealed tube neutron generator. A slow neutron detector monitors the slow neutrons as they re-emerge from soil. Above a hydrogen-rich anomaly the slow neutron flux increases, because hydrogen is an extremely efficient moderator. Since low-metallic landmines contain much more hydrogen atoms than a normal dry sandy soil, the NBS method may be used to detect such landmines. Since 1998 different detector systems have been developed and tested. They have demonstrated the feasibility of the NBS method ⁽²⁾. The sensitivity for mine detection of the NBS device can be improved by obtaining an image of the backscattered slow neutrons instead of just counting the number of neutrons, so a hydrogen-rich area may be found much more easily. The above considerations have led to investigate the applicability of an imaging device with a large detection plane close to the soil^(3,4). To evaluate the influence of various parameters on the performance of the neutron backscattering detector, Monte Carlo simulations were carried out. For these simulations the Monte Carlo simulation MCNP4B code was used. To include the neutron interactions down to slow energies, MCNP4B was run in neutron transport mode only. The neutron cross section data used for these simulations was obtained from the ENDF/602 library ⁽⁶⁾.

METHODS

1- Detection System:

The geometry that was used for these simulations is shown in Figure 1. The detection system consists of sixteen positions sensitive thermal neutron Helium-3 tubes (aluminum tubes, length: 50 cm, diameter: 2.54 cm, tube pitch: 34 mm). The spatial resolution in the detector plane is in the direction perpendicular to the tubes of course equal to the tube pitch (34 mm), and in the direction parallel to the tubes equal to the tube length divided by the number of bins, so $500/16 = 31$. This

Authors Emails: ali_ma602001@yahoo.com, aliali@jazanu.edu.sa

resolution is sufficient to “see” all sizes of land mines. The mine image as simulated by the detector does not reflect the actual mine shape or size, but it always draw a circular with a diameter of around 15 cm. This is explained by the large distance the slow neutron can drift underground before emerging at the surface. Smaller mines produce a spot with only slight smaller diameter, but the mine depth and the distance of the detector from the ground surface (standoff distance) also influence the shape of the image⁽¹⁾. The detection system, AP mine and neutron source are shown in Fig 1.

2- MCNP4B Code:

Monte Carlo N-Particle Transport code (MCNP) version 4B⁽⁵⁾ has been used for simulating this study. MCNP 4B code was executed for a point source in infinite medium. Since the problem is dealing with neutron interaction with the AP mine samples, MCNP 4B code was run in neutron transport mode only. The source strength is assigned to unity to represent a normalized source. The neutron weight factor is 1 in all cells and zero in the cutoff region (outside the boundary surface of the problem). The neutron source was considered to be mono-energetic point source of energy 2.45 MeV to simulate a D-D neutron generator located over the detection system and at its center. F4 Tally (average flux over detector cells) is concerning with total cross section.

3- Anti-Personnel landmine:

The anti-personnel landmine type DLM2 is of cylinder shape of 8 cm diameter and 3.4 cm height filling with TNT simulator and Lucite shell material. A Full description of anti-personnel landmine type DLM2 is listed in table 1^(1,2).

Table (1): DLM2 mine description.

| Mine | Anti-personnel (DLM2) |
|------------------|-----------------------|
| Outer diam. | 8 cm |
| Outer height | 3.4 cm |
| Inner diam. | 7 cm |
| Inner height | 2.2 cm |
| Filling Material | TNT simulator |
| Shell material | Lucite |
| Filling weight | 100 |
| Shell weight | 100.9 |
| Filling H-atom | 1.52E+24 |
| Shell H-atom | 4.86E+24 |

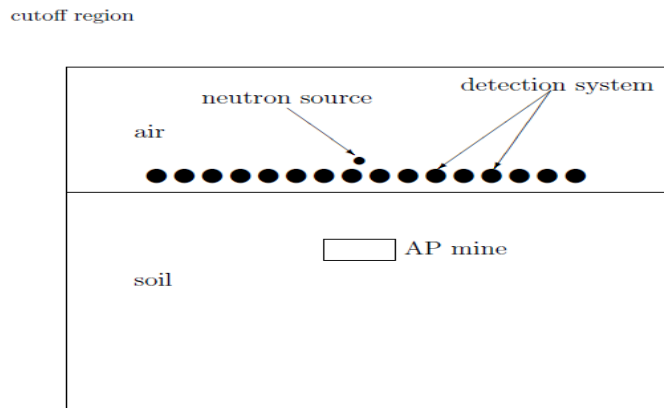


Fig. (1): Schematic diagram of the simulated experiment

RESULTS AND DISCUSSIONS

The simulated constructed images of reflected slow neutrons from AP-mine for different depths and position are presented and discussed in this section. Also, the calculated average neutron flux per particle for different depths and horizontal positions are displayed and discussed.

The response of the DLM2 mine positioned at the center (at coordinates 0,0 cm) of the detector and buried at different depths is shown in Fig. 2. Figure 2 shows the images of scattered thermal neutrons at depths 0 cm, 5 cm, 10 cm and 15 cm respectively. Figure 2.a shows a peak in the center due to the mine. The intensity of this peak decreases as the depth increases from zero to 10 cm as shown in figures 2.b and 2.c. At 15 cm depth the peak disappear as shown in figure 2.d, this means that the AP-mine could be detected if it is buried at depths up to 10 cm.

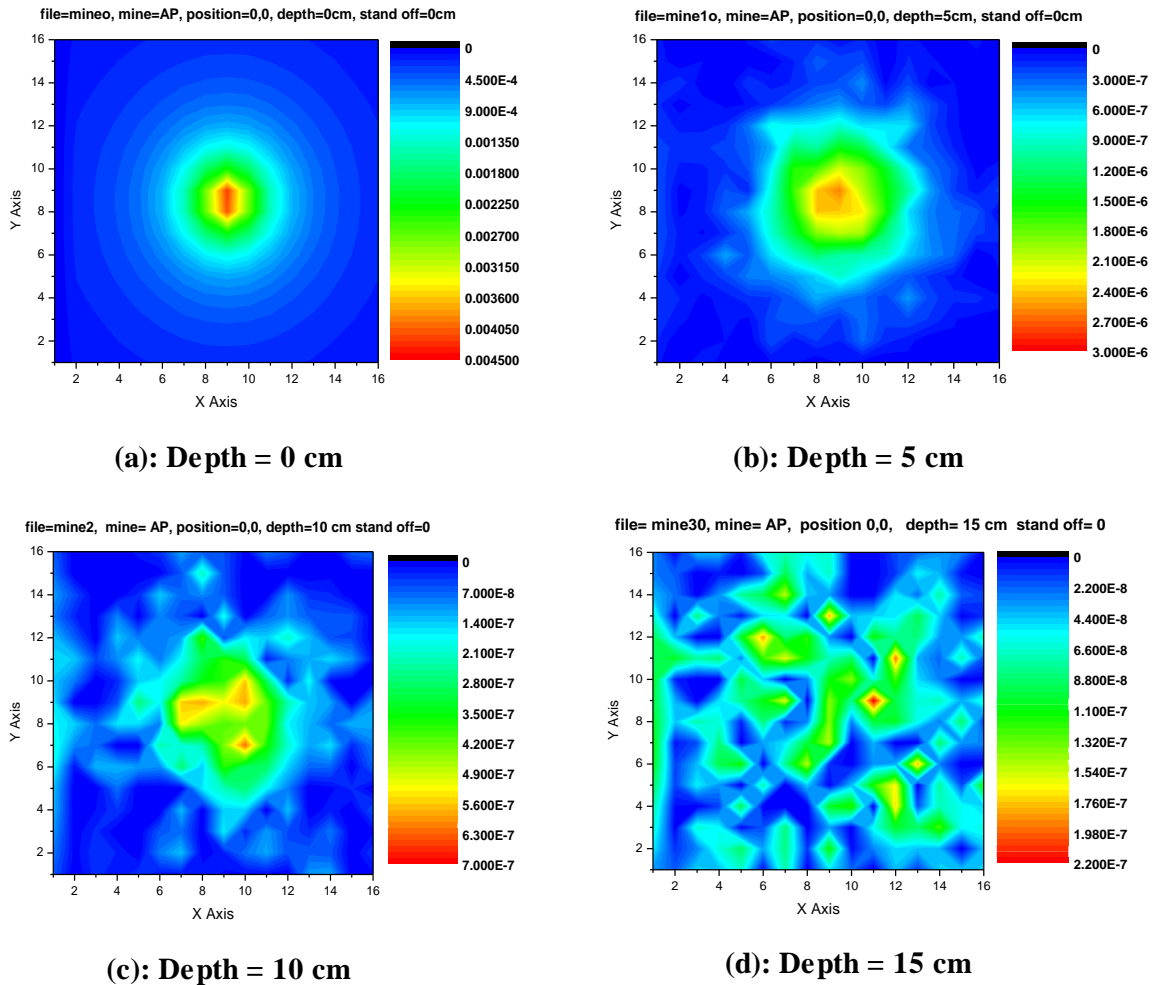


Fig. (2): AP mine images by 2.45 MeV neutrons, the AP mine at the center of the detector and zero standoff distance at different depths

Figure 3 shows the constructed image for AP mine positioned at the side of the detector (at coordinates 0,25 cm) and for different depths. Figure 3.a shows a peak of the scattered neutrons at the top side and the intensity of this peak decreases as the depth increases from zero cm to 10 cm as shown in figures 3.b and 3.c. At 15 cm depth the peak disappears as shown in figure 3.d. It means that the two dimensional He-3 detector can detect the anti-personnel landmine up to 10 cm depth.

Figure 4 shows images constructed from slow neutron backscattered for AP mine positioned at the corner of the detector (at coordinates 25,25 cm) at different depths. Figure 4.a shows a peak of the scattered neutrons at the right top corner of the image and the intensity of the peak decreases as the depth increases from zero cm up to 10 cm as shown in figures 4.b and 4.c. At 15 cm depth the peak disappears as shown in figure 4.d. It means that the two dimensional He-3 detector can detect the anti-personnel landmine up to 10 cm depth.

Figure 5 shows the relation between average slow neutron flux (neutron/cm²) per neutron and the landmine depths. The landmine is at the center of the detector. The average neutron flux per particle is 3.458e-4 n/cm² when the landmine exists at the surface of the earth. When the landmine is buried at 5 cm, the average neutron flux is reduced to 26.8% when the landmine is at the surface and is reduced to 7.5% When the landmine is buried at 10 cm. at 15 cm depth the average neutron flux is reduced to 3.7%.

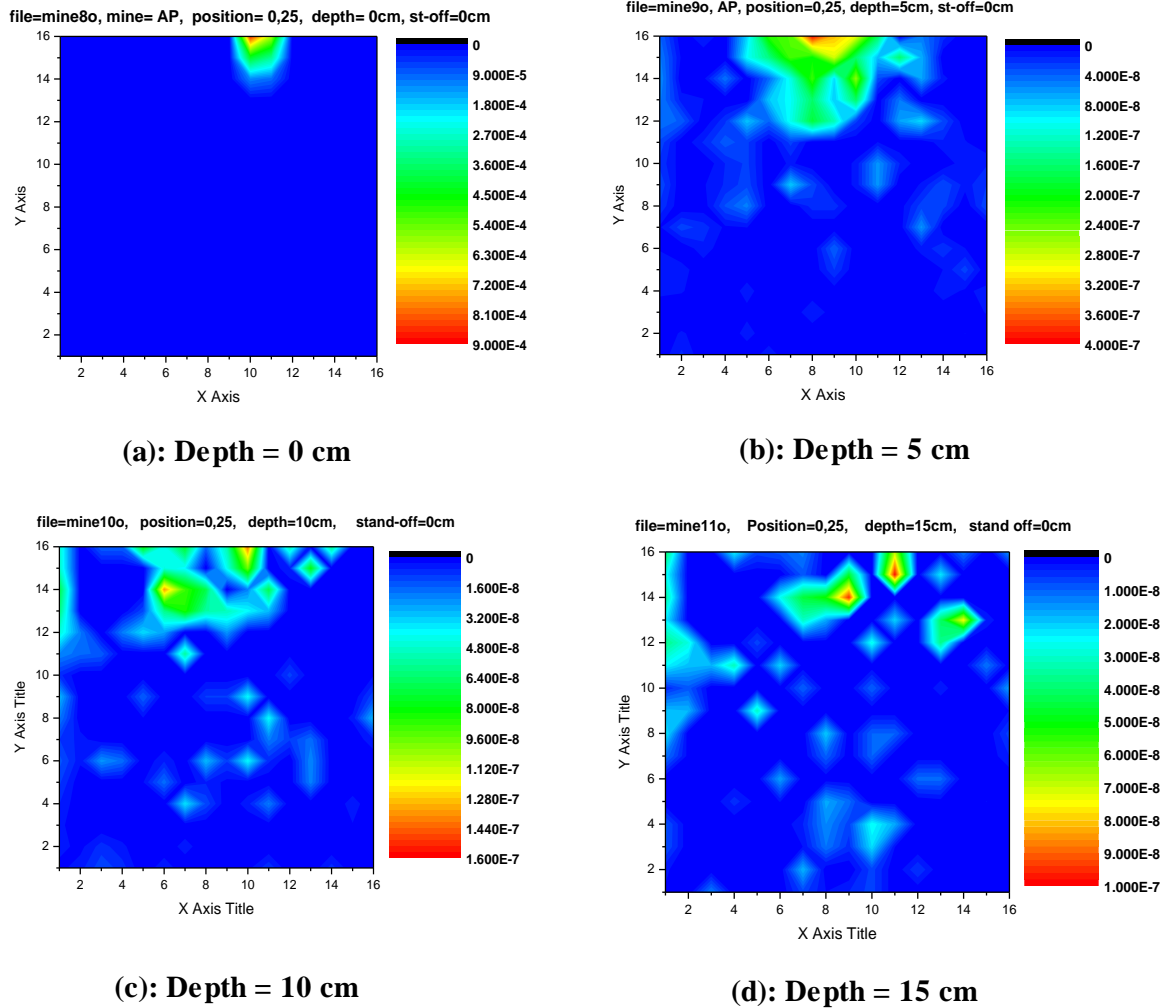


Fig. (3): AP mine imaged by 2.45 MeV neutrons, the AP mine at the side of the detector and zero standoff distance at different depths.

Figure 6 shows the relation between the average slow neutron flux (neutron/cm²) per neutron and the AP landmine depths when the landmine at the side of the detection system. The average slow neutron flux per particle is 1.62487e-5 n/cm² when the landmine exists at the surface of the earth. When the landmine is buried at 5 cm, the average neutron flux is reduced to 45% out of that for the landmine at the surface and is reduced to 17.3% when the landmine is buried at 10 cm. At 15 cm depth the average neutron flux is reduced to 10%.

Figure 7 shows the relation between the average slow neutron flux (neutron/cm²) per neutron and the landmine depths for landmine exists at the corner of the detection system. The average slow neutron flux per particle is 5.26143e-6 n/cm² when the landmine exists at the surface of the earth. When the landmine is buried at 5 cm, the average neutron flux is reduced to 41.6% out of that when it is at the surface and is reduced to 23% when the landmine is buried at 10 cm. At 15 cm depth the average neutron flux is reduced to 15.2%.

From figures 5,6 and 7 one can deduce that when a landmine exists at the side of the detection system, the average neutron flux is reduced to 4.59% out of that for a landmine exists at the center of the detection system and is reduced to 1.49% when the landmine position is at the corner of the detection system.

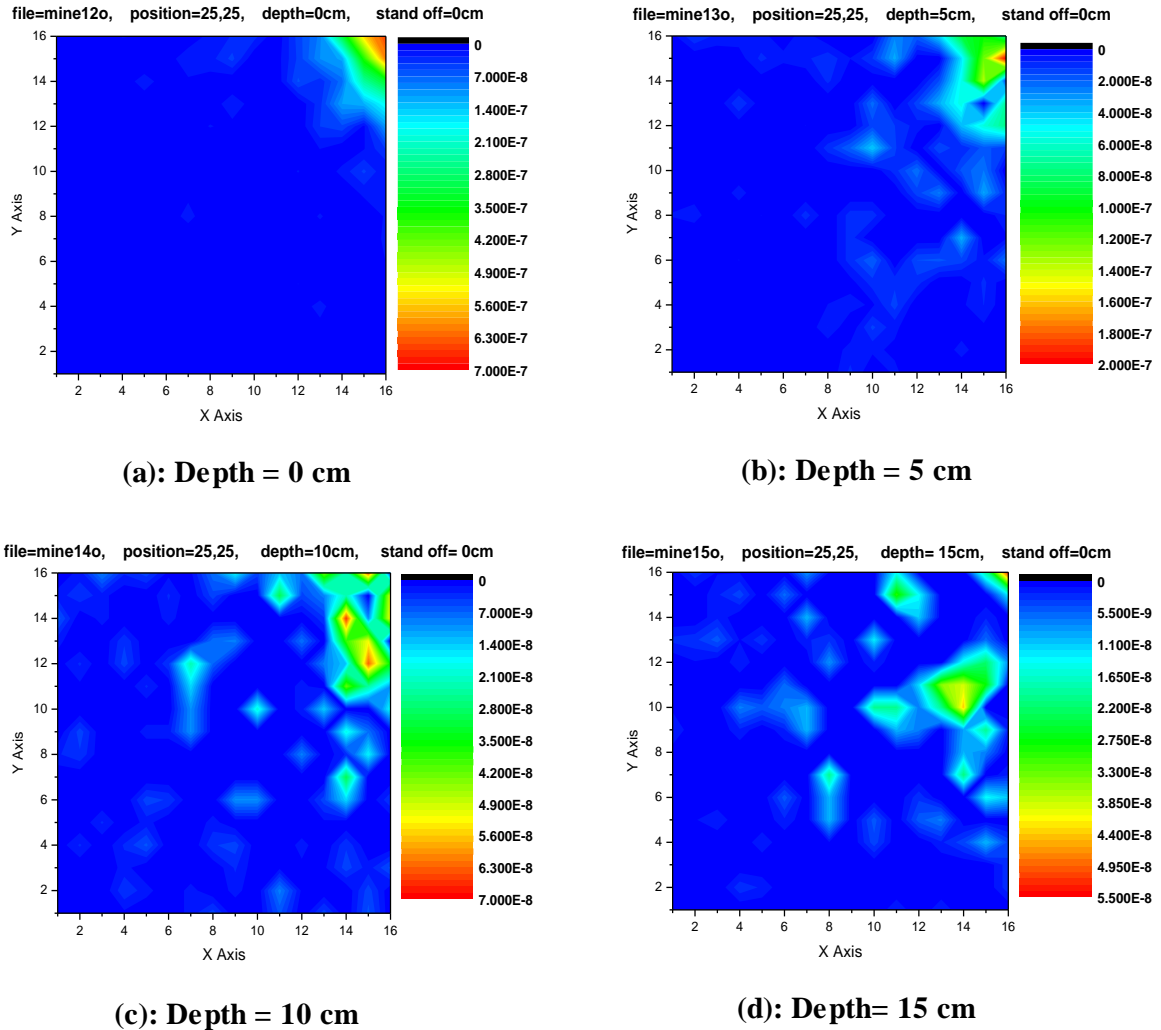


Fig. (4): AP mine imaged by 2.45 MeV neutrons, the AP mine at the corner of the detector and zero standoff distance at different depths.

CONCLUSION

The detection of anti-personnel landmine by neutron backscattering technique can be simulated by using MCNP 4B code. The relative error of these simulations is always less than 1%. The intensity of the scattered neutrons depends on the buried depth and the horizontal position at which the mine exists. The anti-personnel landmine DLM2 can be detected by the 16-He-3 detector system when it is buried in the ground at depth down to 10 cm. When the AP mine buried at the side of the detector, the calculated average neutron flux is reduced to 4.59% out of that when it is buried at the center of the detector and is reduced to 1.49 when it is buried at the corner of the detection system.

ACKNOWLEDGEMENTS

The author would like to thank the team of cyclotron project, Exp. Nuclear Physics department, Nuclear Research Center, Atomic Energy Authority, especially Dr. Ahmed M. M. Solieman, for his help.

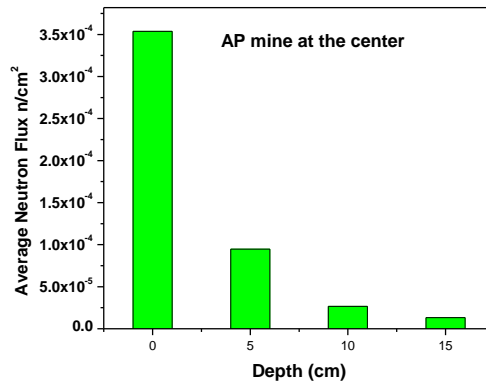


Fig.(5): Total neutron count at different depths for AP mine at the center of the detector

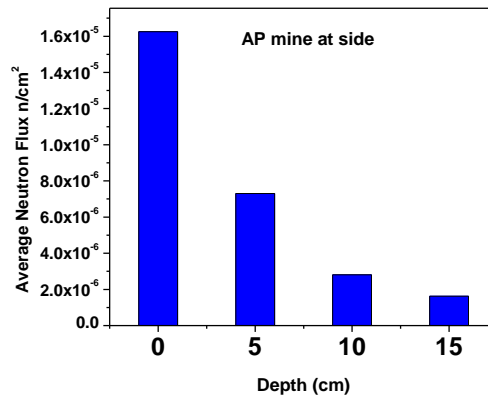


Fig.(6): Total neutron count at different Depths for AP mine at the side of the detector

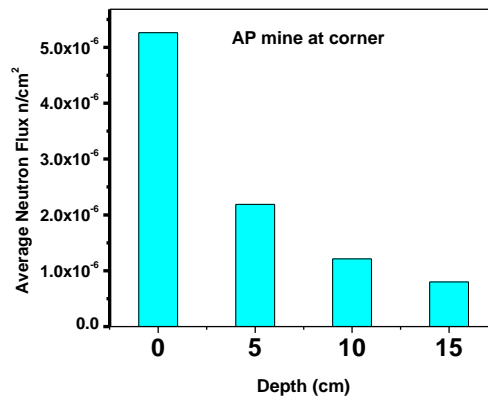


Fig.(7): Total neutron count at different Depths for AP mine at the corner of the detector

REFERENCES

- (1) A Feasibility Test of Land Mine Detection in a Desert Environment Using Neutron Back Scattering Imaging, Victor Bom, A. Mostafa Ali, A. M. Osman, A. M. Abd El-Monem, W. A. Kansouh, R. M. Megahid, and Carel W. E. van Eijk, IEEE TRANSACTIONS ON NUCLEAR SCIENCE, VOL. 53, NO. 4, AUGUST 2006, P. 2247- 2251.
- (2) DUNBID, the Delft University neutron backscattering imaging detector, V.R. Bom, C.W.E. van Eijk, M.A. Ali, Applied Radiation and Isotopes 63 (2005), P. 559–563.
- (3) Land Mine Detection With Neutron Back Scattering Imaging Using a Neutron Generator, Victor Bom, Mostafa A. Ali, and Carel W. E. van Eijk, IEEE TRANSACTIONS ON NUCLEAR SCIENCE, VOL. 53, NO. 1, FEBRUARY 2006, P. 356- 360.
- (4) Experimental results and Monte Carlo simulations of a landmine localization device using the neutron backscattering method, C.P. Datema*, V.R. Bom, C.W.E. van Eijk, Nuclear Instruments and Methods in Physics Research A 488 (2002) P. 441–450.
- (5) MCNP – A General Monte Carlo N-Particle Transport Code-Version 4B, Los Alamos National Laboratory Report LA-12625-M. Briesmeister, J.F., 1997.
- (6) Endf/B-VI library generation and testing for the scale code system, M.E. Dunn, P. B. Fox, N. M. Greene and L. M. Petrie, 2005 ANS annual meeting, San Diego, California, June 5-9, 2005